Earth Observation and Geomatics Engineering 1(1) (2017) 16–25

EARTH OBSERVATION AND GEOMATICS ENGINEERING

website: https://eoge.ut.ac.ir

Automatic generation of E-LOD1 from LiDAR point cloud

Maryam Sajadian, Hossein Arefi *

School of Surveying and Geospatial Engineering, College of Engineering, University of Tehran, Tehran, Iran

Article history:
Received: 04 December 2016, Received in revised form: 6 April 2017, Accepted: 18 April 2017

ABSTRACT

LiDAR as a powerful system has been known in remote sensing techniques for 3D data acquisition and modeling of the earth's surface. 3D reconstruction of buildings, as the most important component of 3D city models, using LiDAR point cloud has been considered in this study and a new data-driven method is proposed for 3D buildings modeling based on City GML standards. In particular, this paper focuses on the generation of an Enhanced Level of Details 1 (E-LOD1) of buildings containing multi-level flat-roof structures. An important primary step to reconstruct the buildings is to identify and separate building points from other points such as ground and vegetation points. For this, a multi-agent strategy is proposed for simultaneous extraction of buildings and segmentation of roof points from LiDAR point cloud. Next, using a new method named "*Grid Erosion*" the edge points of roof segments are detected. Then, a RANSAC-based technique is employed for approximation of lines. Finally, by modeling of the rooves and walls, the 3D buildings model is reconstructed. The proposed method has been applied on the LiDAR data over the Vaihingen city, Germany. The results of both visual and quantitative assessments indicate that the proposed method could successfully extract the buildings from LiDAR data and generate the building models. The main advantage of this method is the capability of segmentation and reconstruction of the flat buildings containing parallel roof structures even with very small height differences (e.g. 50 cm). In model reconstruction step, the dominant errors are close to 30 cm that are calculated in horizontal distance.

KEYWORDS

Point cloud
Building extraction
Edge detection
Line approximation
3D reconstruction
Multi-level flat-roof building

1. Introduction

Three dimensional city modeling is a geometric reconstruction and 3D graphical representation of objects in urban areas such as ground, buildings, streets, and vegetation. Buildings, as main elements of 3D city models, can be reconstructed based on a wide range of techniques in acquisition, classification, degree of automation and analysis of data derived from, e.g. laser scanners, aerial photogrammetry, and cadastral information. (Jürgen et al., 2005). Current methods usually model the roof shapes and footprints of buildings and display the buildings in geometric and visual forms using these information (Haala & Kada, 2010). Maas and Vosselman (Hans-Gerd & Vosselman, 1999) proposed a model-driven method by derivation of house model parameters from invariant moments. Alharthy and Bethel (Alharthy & Bethel, 2002) proposed a method for reconstruction of prismatic model of buildings. In another paper, they have separated planar roof facets and reconstructed the building model based on estimated geometric surface parameters (Alharthy & Bethel 2004). A projection based approach for 3D model generation of the buildings was proposed by Arefi et al (Arefi et al., 2008). Kabolizade et al. (Kabolizadeh et al., 2012) proposed a model-driven approach for 3D building reconstruction from LiDAR data based on genetic algorithm. Satari et al. (Satari et al., 2012) used the combination of the data-driven and model-driven methods for reconstruction of cardinal planes and appended parts on roof. In the other study, separation of ground points and building detection is achieved by using features' geometry and regional attributes (Satari et al.,

* Corresponding author

E-mail addresses: m.sajadian@ut.ac.ir (M. Sajadian); hossein.arefi@ut.ac.ir (H. Arefi)

DOI: 10.22059/eoge.2017.230917.1004

2012). Song et al. (Song et al., 2015) proposed an automatic method for extraction and reconstruction of buildings with curved rooves. Many methods have been studied to combine LiDAR data and roof images for building reconstruction such as (Ye et al., 2010 ; Awrangjeb et al., 2013 ; Li et al., 2013). Arefi and Reinartz (Arefi & Reinartz, 2013) employed the extracted edge information from the ortho-rectified Worldview–2 images as an additional source of information for precise 3D building reconstruction. The use of cadastral maps as the additional data resource is usually for the separation of building points from other data points (Hala & Brenner, 1999), (Alexander et al., 2009), and (Kada & McKinley, 2009). According to City Geography Markup Language (City GML) standard, five consecutive Levels Of Details (LOD) are defined. LOD1 is dedicated to a 3D building model shaped using a single height flat roof structures. The LOD2 model enables representing the parametric roof shapes such as gable and hip models (Arefi & Reinartz, 2013). In spite of the fact that the flat roof buildings in big industrial cities include multi-level roof structures with different elevation levels, the LOD1 models the buildings as cubic shapes with the same height values for all roof planes. An example of a flat roof building with multi-level structures is shown in Figure 1. The 3D building reconstruction of such buildings are often more difficult than the tilted-roof buildings because of the same normal vectors and parallel roof's planes. In addition, the boundaries of planes in sloped buildings can be extracted by intersection of planes. But this is not applicable in the flat building containing multi-level rooves. Because of these problems and limitations, in this paper a method is presented to generate a more realistic model of multi-level flat roof buildings (E-LOD1) as well as a 3D modeling of tilted-roof buildings (LOD2).

2. Proposed Method

The workflow of proposed method is shown in Figure 2. There are four steps for 3D building reconstruction, namely: simultaneous building extraction and segmentation, edge detection, line approximation, and the 3D modeling. The details of each step are explained in the following sub-sections.

2.1 Simultaneous building extraction and segmentation

A multi-agent method is proposed for extraction of buildings from LiDAR point cloud and segmentation of roof points at the same time which is described in details in the next subsections.

2.1.1 Extraction of ground and vegetation candidate points

Ground candidate points often have the lowest height values among all the points. Therefore, the height threshold can be used by local minimums for extracting these points. In this process, the objects with low height values such as vegetation, ground, roads, and similar points are separated

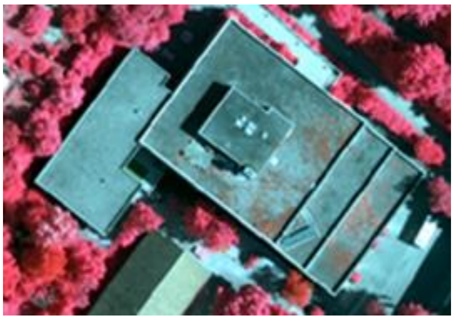

Figure 1. Multi-level flat-roof building

from other data. Since the laser pulse can be passed through the vegetation and collide with the ground or object under vegetation and two (first- and last-pulse) or more pulses can be recorded, this property can be used to extract some points of vegetation covers. More explanations are given in (Sajadian & Arefi, 2014).

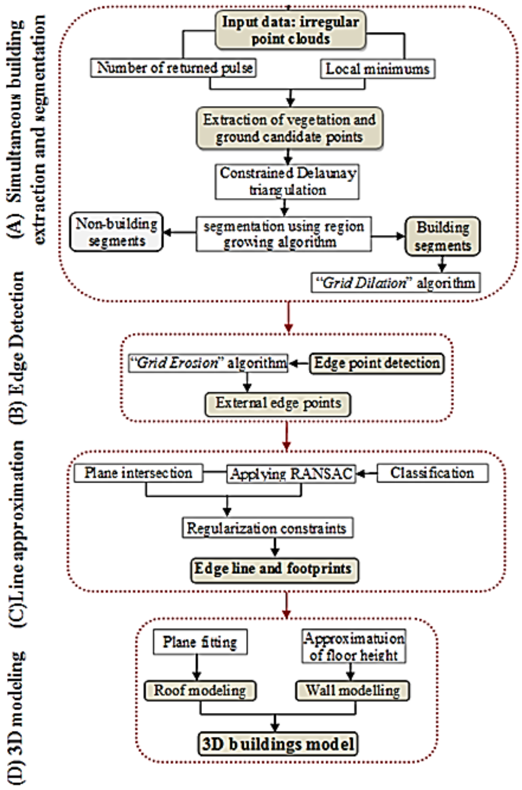

Figure 2. Workflow of proposed method

2.1.2 Constrained Delaunay Triangulation

In previous step, the extracted ground and vegetation candidate points are removed from raw LiDAR data. In this step, the neighborhood relation between points is established using Delaunay triangulation. Then, a threshold is applied for removing the triangles connecting the edges between different objects or multi-level structures. Accordingly, if at least one of the sides of the triangle has the length larger than τ (Mian et al., 2004), it is classified as the triangle connecting the edges and must be removed (Figure 3).

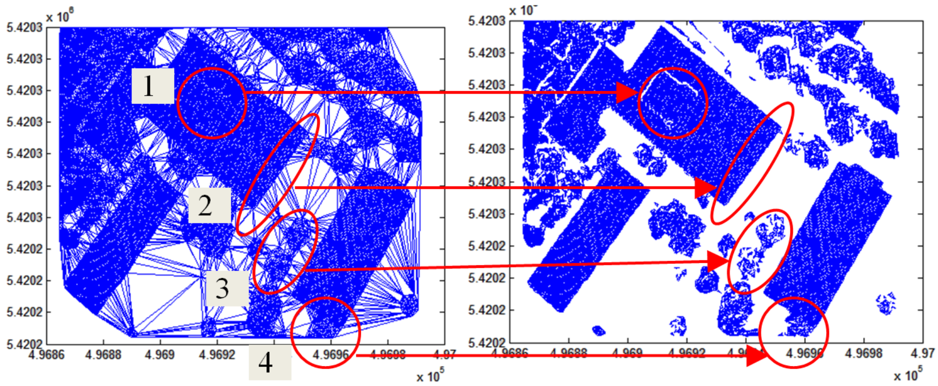

Figure 3. Constrained Delaunay Triangulation

The threshold τ is calculated by Eq. (1):

$$\tau = \bar{s} + t\mu \quad (1)$$

where, $\bar{s}$, t, and μ are the means of the length of the triangle's sides, standard deviation factor and standard deviation of the length of the triangle's sides, respectively. The standard deviation can vary between 0 - 3. Experimentally, the appropriate value of t can be between 0.3 - 0.7. Eq. (1) is used for first time in this paper to improve the results of the multi-level flat-roof buildings segmentation. In Figure 3 area 1, the triangles connecting the two levels of the flat building have a length more than threshold by Eq. (1) and are removed. Removing these triangles is very important and it makes proper separation of parallel levels with different height values. In area 2, the triangles connecting the edge of the building and surrounding region and trees are removed. In area 3, due to the height difference between the tree points, many triangles are removed and some small areas are created which are useful to extract the segments of trees. In area 4, because of small height difference between the roofs and tall trees, the neighboring triangles cannot be removed easily. In the next step, these tree points will be removed from roof points using normal vector criteria.

2.1.3 Segmentation

Here, the objectives of segmentation are to label the points belonging to the same plane, to detect the remained non-building points more especially trees points, and to extract the building segments. Triangles which belong to the same plane have same normal vector direction. This property is used to segment all the points. Unit normal vector of each triangle is calculated by external multiplication of two vectors $\overrightarrow{v1}$ and $\overrightarrow{v2}$ by Eq. (2).

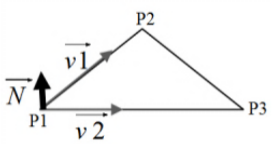

$$\vec{N} = \frac{\overrightarrow{v1} \times \overrightarrow{v2}}{|\overrightarrow{v1} \times \overrightarrow{v2}|} \quad (2)$$

First, for each triangle three neighboring triangles according to its three sides are determined. A region growing algorithm starts working with a random triangle (s.t). Three neighboring triangles of this triangle are considered and angle between unit normal vector of them ($\vec{N}_{c.t}$) and random triangles ($\vec{N}_{s.t}$) is calculated by Eq. (3):

$$\theta = \cos^{-1}(\overrightarrow{N_{s.t}} \bullet \overrightarrow{N_{c.t}}) \quad (3)$$

If θ is smaller than predefined angle threshold, related triangle (c.t) will be added for segmentation of random triangle and the neighboring triangles of this triangle are considered. This process continues until all triangles that satisfy this limitation are set to be of same segment. Next, region growing algorithm continues by another random triangle which is selected among remaining triangles until all triangles are segmented (Figure 4 left). Experimentally, the appropriate value of θ is between 15-18 degrees. Large segments that have an area larger than the defined threshold are set to be as buildings. So the building points are extracted and segmented with the removal of non-building points, simultaneously. Segmentation results are shown in Figure 4. In this process, the non-belonging roof features (e.g. areas 1 and 2) as well as the tall trees close to building rooves (e.g. area 3) are also removed. Also, through segmentation process, the noises are removed. Because noises create the big triangles having long sides which eventuate in small segments.

2.1.4 Segment labeling

In previous step, building segments are detected, but it is necessary to detect segments belonging to the same building. For this, segments are labeled using a new method named *"Grid Dilation"*. The process is named Grid Dilation because of using the morphological dilation operation which is applied on a regular grid. The proper grid size is 0.5 m experimentally. Each segment in 3D space is considered, imaginary grid is laid over it and 3D coordinate of grid nodes with nearest neighbor method are determined. So, segments are converted from vector to raster space and accordingly image processing techniques can be employed. Gaps must be filled and then the dilation operation is applied on each grid.

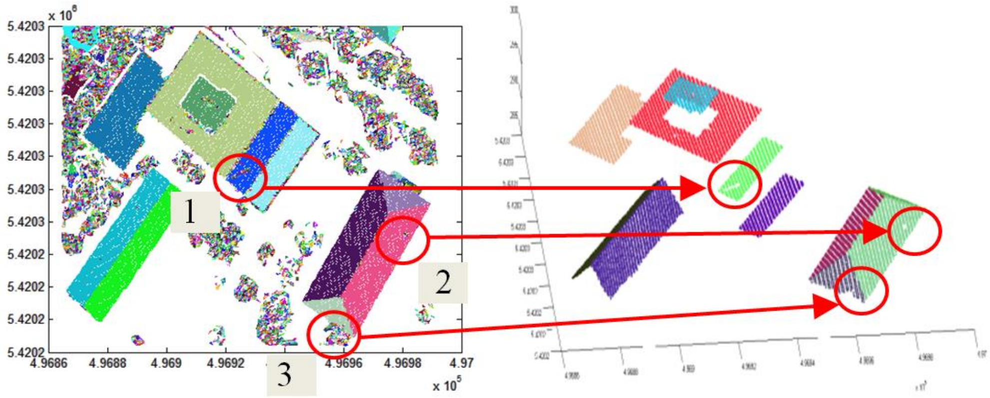

Figure 4. Left (Segmented triangles, right) Building segments points

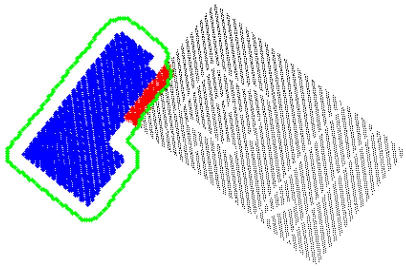

Figure 5. Grid Dilation: points of being processed segment (blue), edge points of dilated grid (green), neighboring points (red)

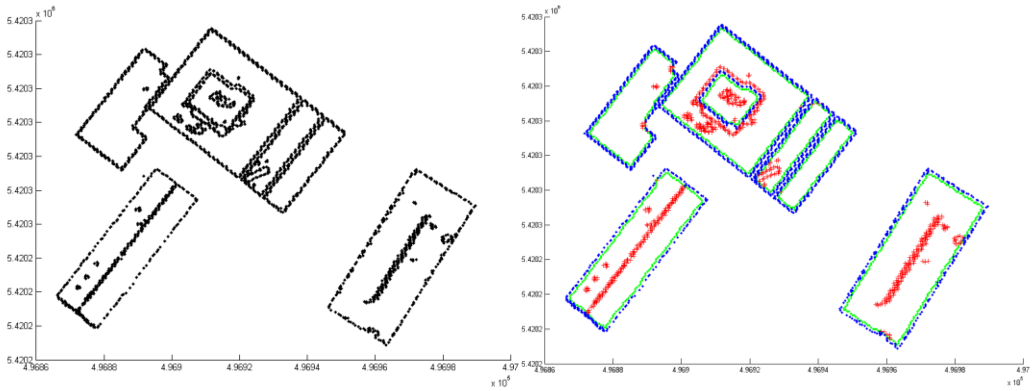

Figure 6. Left) primary edge points, Right) *Grid erosion*: edge points of: eroded grid (green), internal (red), final (blue)

By using this process, the grids will be pulled up or overspread. Then, the edge of dilated grid is detected (green points in Figure 5). The segments belonging to those points that are inside this closed boundary are known as neighboring segments. All neighboring segments are merged to generate a unique building.

2.2 Detection of edge points

After extracting the building segments, the edge points of each segment can be detected. Points of triangles having no neighboring triangles are extracted as edge points (Figure 6 left). As shown in (Figure 5 red circles), in the extraction process, the noises, external objects, and tree points on the rooves are removed. This is an advantage of the proposed method, however it leads to the creation of undesired edge points. These undesired edge points are known as internal points and must be removed. In this paper, a method named "*Grid Erosion*" is employed for removing these internal points and finding the real edge points.

"*Grid Erosion*": it is like the Grid dilation method, but here Erosion operation is used instead of Dilation operation. By using this process, the grids will be shrunk or compressed. Then, the edge of eroded grid is detected. The edge points are used for separating internal and external edge points. So all points in the vector space that are inside this closed boundary, are known as internal or undesired edge points which should be removed. As shown in Figure 6, "*Grid Erosion*" could successfully extract the external edge points in vector space.

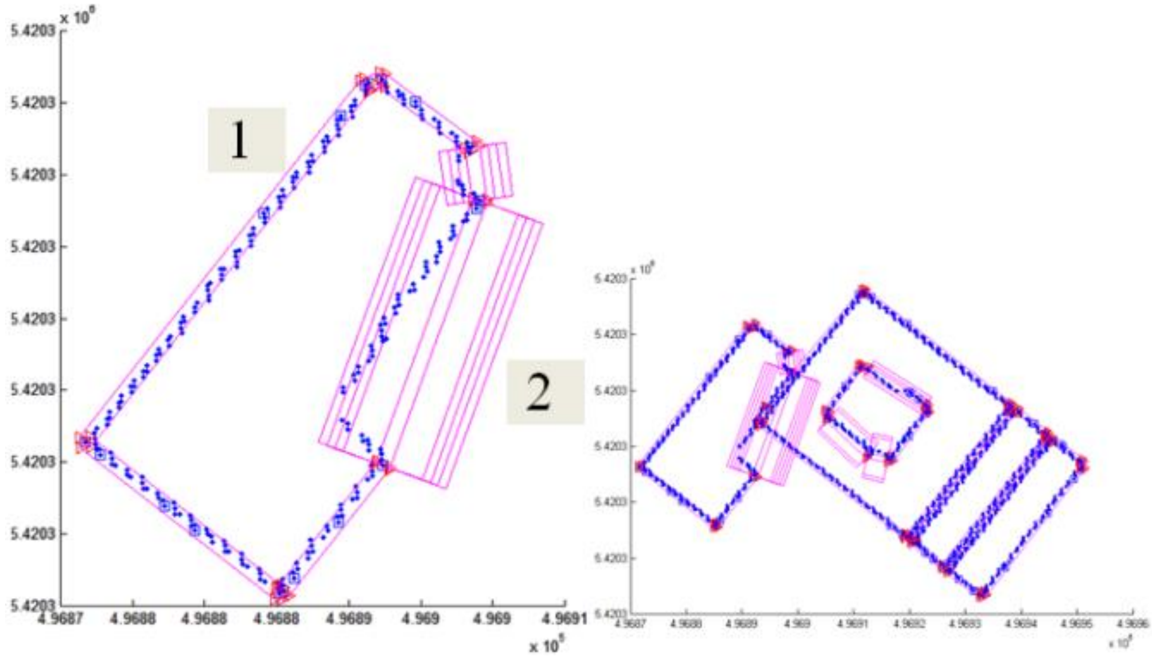

Figure 7. Classification of edge line: Convex (1) and non-convex (2) line segments

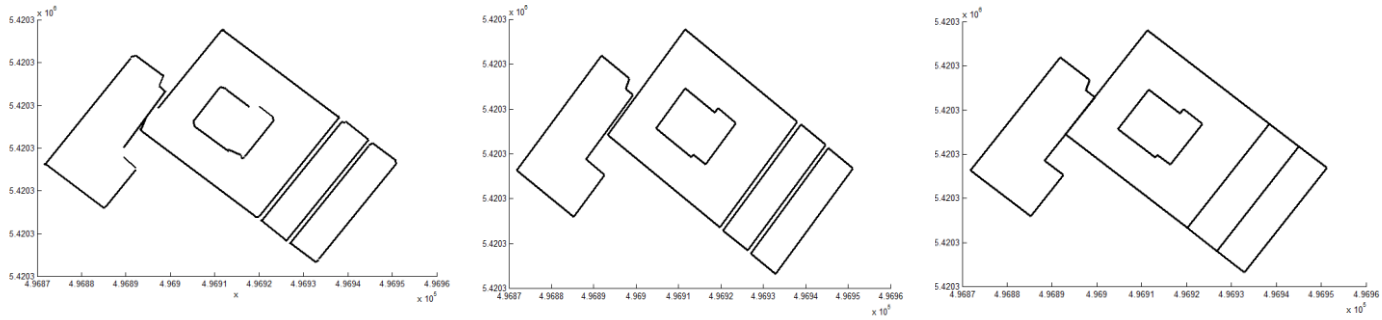

Figure 8. Approximated lines: primary lines (left), applying regularization constraints (middle), incorporation of segments (right)

2.3 Line approximation

After detecting the final edge points, the RANSAC algorithm is employed (Fischler & Bolles, 1981) to approximate building lines. RANSAC is a powerful technique in line fitting. Basically, it is not possible to use the least square method in data that contains more than one line. But it is possible to approximate the lines near the ground-truth using RANSAC algorithm iteratively. In this technique, parameter selection plays a very important role in order to reach correct results. It can be stated explicitly that the achieving of the best parameters using trial and error procedure is onerous and time consuming. In order to reduce the sensitivity of RANSAC to select the parameters and eliminate the need for heavy post-processing, the edge points are grouped. In the first step, the convex point of each segment is determined. A line is created by connecting any two consecutive convex points and the angle between these lines is calculated. If the angle is smaller than the predefined threshold, it belongs to a unit segment lines. A threshold of about 13-17 degrees is appropriate. This process is repeated for all lines in order to detect all convex points belonging to the same line. The next step is the determination of all edge points belonging to each classified line. For this, the first and last convex points of every line segment are determined. Then, a rectangle is inscribed by the points. The inner edge points of this rectangle are known as edge points of each line segment (Figure 7). If the number of edge points of each line segment is to be named n and the length of the corresponding line to be named l, while the ratio of n to l be smaller than predefined threshold, this line segment is set to be as a non-convex line segment. In this case, the line segment consists of several lines (Figure 7 area 2). Otherwise, it is known as a convex line segment (Figure 7 area 1). After identifying the non-convex parts, the threshold (width of rectangle) in certain steps, e.g. 1 meter, is increased until the ratio of n to l is satisfied. This process is performed for each segment independently. After the classification of the edge points, a RANSAC algorithm is separately applied on each classified edge-points group. For the non-convex lines segment, the process must be repeated until all lines are extracted. After applying the RANSAC algorithm, primary lines are generated (Figure 8 left). The regularization constraints should be applied on primary lines to generate the final lines. The main regularization constraints are: (1) To remove the small lines, (2) Apply parallel condition on all lines by changing the direction of the weighted average azimuth, (3) Merge the lines close to each other, (4) Connect two consecutive parallel lines with an orthogonal line, and (5) Intersect the crossover lines. The mentioned algorithm is proposed specially for line approximation in multi-level flat buildings. For buildings with tilted rooves, the roof planes are usually intersected to generate the internal boundaries. The results are achieved with so many repetitions. Regularization constrains are repeated after any change. The main results are given in Figure 8.

2.4 3D modeling

3D modelling can be done in two steps: roof and wall modeling. For this, all points of each building segment in a 3D space are considered and a plane is fitted to these points using the least square technique. The height values of the start and end points of each line are measured according to the equation of fitted plane. So, the roof models can be reconstructed using this information. For the reconstruction of wall models, it is necessary to approximate the height values of floor. The morphological dilation is used for finding the points around buildings. The average of minimum height values is determined as floor height. At the end, roof boundary points are projected on the floor building. The wall models can be reconstructed using wall and floor points.

3. Result and discussion

The proposed algorithm for 3D reconstruction of building models has been implemented in urban areas over Vaihingen city, Germany. The average point density of input data is about 4 pts/m2. The final 3D models of reconstructed buildings in Area 1 are shown in Figure 9. Also, the algorithm is applied on an area comprised multi-level flat buildings (Figure 10). The results of the implemented steps are listed below.

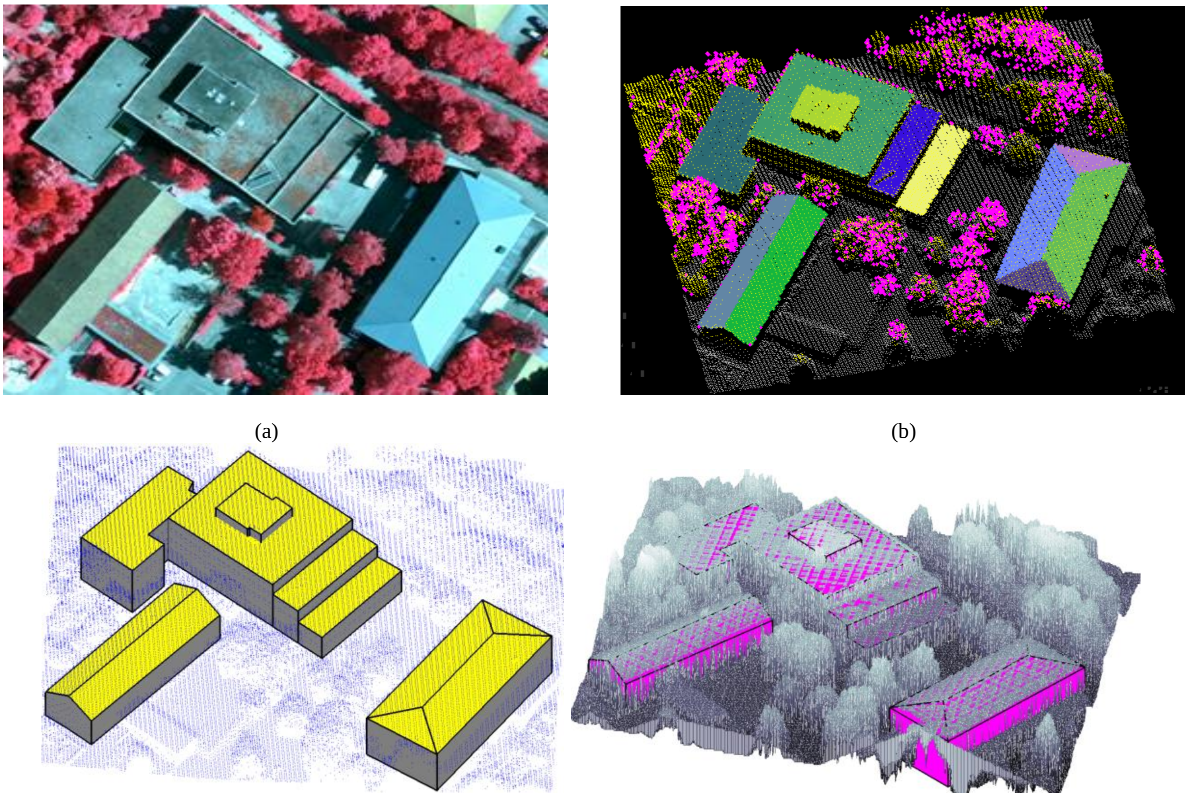

(a) (b) (c) (d)

Figure 9. 3D models of buildings in area 1: (a) aerial image, (b) building segments, (c) buildings model on point clouds, (d) buildings models on DSM

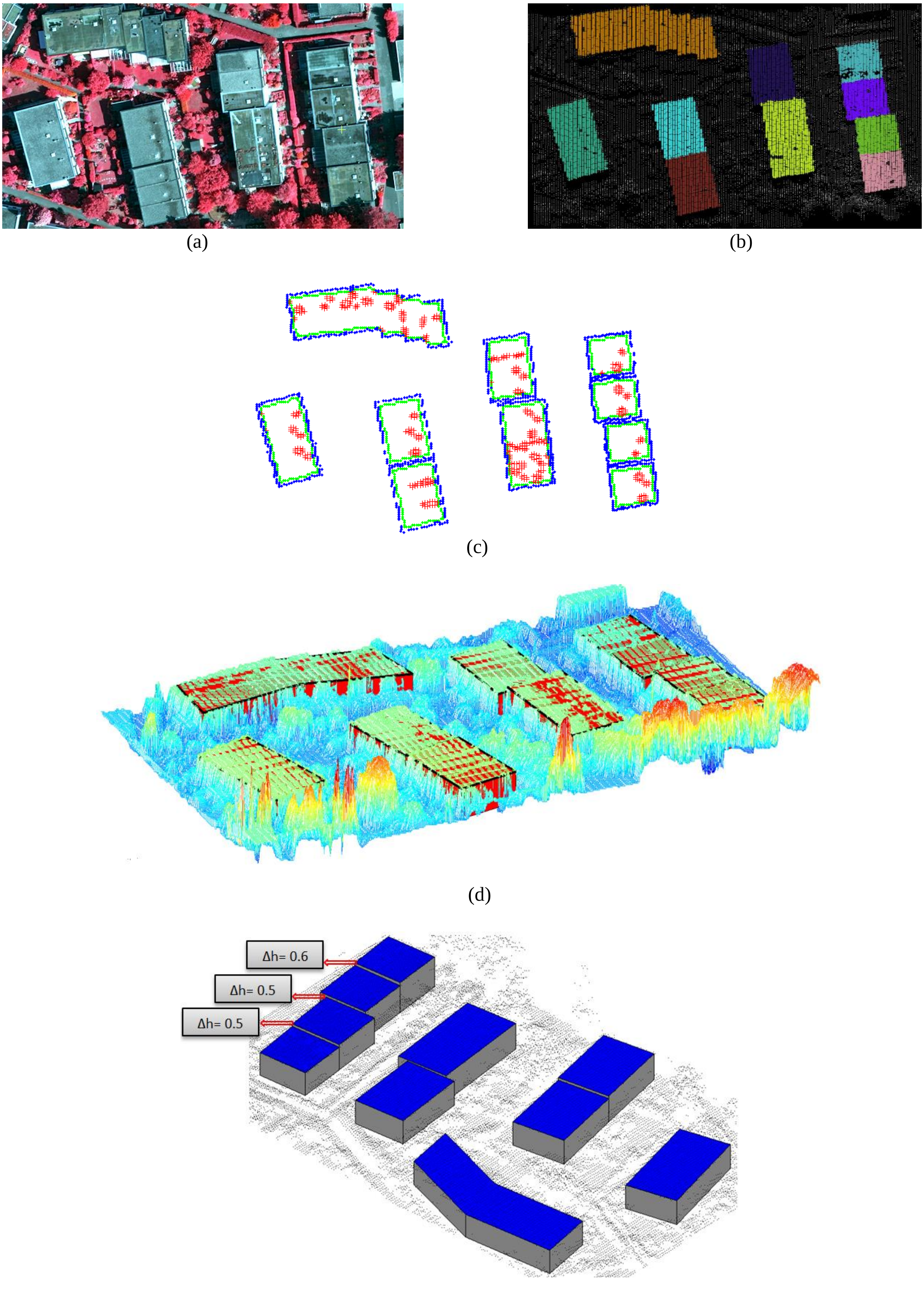

Figure 10. Enhanced LOD1 (E-LOD1) of buildings in area 2: (a) aerial image, (b) building segments, (c) edge points, (d) buildings model on DSM, (e) buildings model on point clouds

Table 1. Quantitative assessment in areas 1 and 2

Building	Errors (m)	Mean (m)	Std. Dev. (m)
	0.18, 0.38, 0.37, 0.17	0.27	0.11
	0.45, 0.48, 0.41, 0.39, 1.10, 0.68, 0.46, 0.48, 0.44, 0.68, 0.82, 0.53, 0.26, 0.36, 0.60, 0.63, 0.46, 0.42, 0.35, 0.29	0.43	0.19
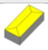	0.29, 0.32, 0.33, 0.30	0.31	0.02
	0.33, 0.46, 0.30, 0.12	0.30	0.14
	0.22, 0.38, 0.35, 0.22, 0.05, 0.36, 0.35, 0.13	0.26	0.12
	0.22, 0.24, 0.43, 0.25, 0.30, 0.39, 0.41, 0.14	0.30	0.10
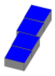	0.30, 0.52, 0.15, 0.15, 0.13, 0.45, 0.13, 0.26, 0.45, 0.29, 0.29, 0.18, 0.43, 0.57, 0.20, 0.29	0.30	0.14
	0.89, 0.34, 1.33, 1.41, 1.53, 1.83	1.22	0.53

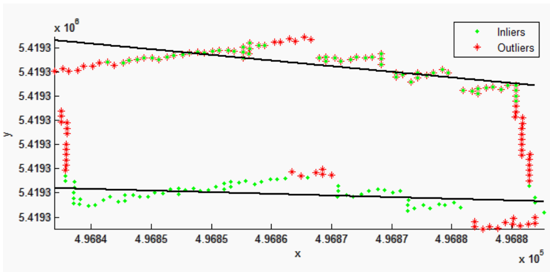

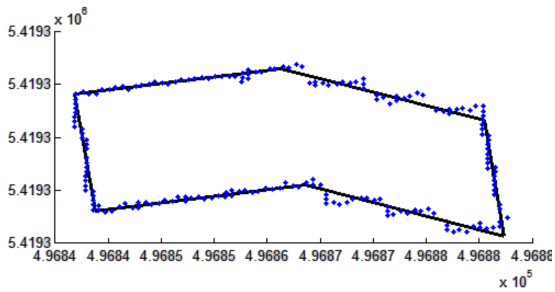

Figure 11. Line approximation: Approximated lines using basic RANSAC (left), approximated lines using proposed method (right)

3.1 Detection and separation of building segment

As mentioned before, the most existing approaches were faced with difficulties in separating the parallel planes, while the proposed methods could identify all segments of multi-level flat buildings even with very small height differences (e.g. 50 cm in Figure 10).

3.2 Edge detection

In this study, the "*Grid Erosion*" algorithm was proposed for detection of edge points. This method can automatically extract undesired or internal edge points.

3.3 Estimation of roof planes

The visual assessments of the final models and the DSM comparison (Figures 9 and 10) show that the buildings' planes are successfully estimated using the least square method and located on the correct positions. In the proposed method, the plane fitting process can be done with high precision by removing the external objects and trees on the buildings' rooves and noises.

3.4 Line approximation

The results show that the approximations of small lines are possible by classification of the edge points before applying RANSAC algorithm. But, one building in the area 2 is an exception and small lines of this building cannot be approximated correctly. However, the approximated lines are better than the results of the basic RANSAC algorithm (cf. Figure 11).

Due to the lack of access to a ground truth, building roof model is digitized from LiDAR point clouds manually and compared with the resulted roof models for a quantitative assessment. The height differences between the corner points are compared as indicated in Table 1.

Table 1 shows that in area 1, the quality of the 3D model in gabled and hipped buildings is better than flat buildings. Thin walls of the flat buildings are considered as noises and were removed in the segmentation process. However, removing the thin walls can increase the vertical accuracy while decreasing the horizontal accuracy. Also, Table 1 shows that the dominant errors are close to 30 cm. The errors can be yield from all phases of building extraction, detection of edge points, and line estimation, etc. So, it proves that the methodology leads to very good results.

4. Conclusion

In this paper, a new method is proposed for reconstruction of a 3D building model with flat roof using irregular LiDAR data. Since the low consideration about modeling of multilevel structures can be seen in most of the current studies, it was tried to focus on these buildings in this work. The proposed method is able to separate the parallel and non-parallel planes without dependence on the number of clusters. The quality of the final results directly depends on the length constrain (in Eq. (1)), the triangle neighborhood, and the classification of the edge points. The length constrains and the triangle neighborhood have contributed to the correct segmentation. It is possible to approximate more natural lines in comparison with the basic RANSAC algorithm by pre-classification of the edge points. Another advantage of the proposed method is the removal of interpolation effects, since the algorithm is applied on the original point clouds. Since the LiDAR system cannot record the exact positions of building edges and so, in some cases, the detailed reconstruction of lines is not possible, many researches have been developed to combine the LiDAR data and images to compensate these shortcomings and problems, and increase the precision of the reconstructed 3D models of buildings.

References

Döllner, J., Buchholz, H., Brodersen, F., Glander, T., Jütterschenke, S., & Klimetschek, A. (2005, June). Smart Buildings – A concept for ad-hoc creation and refinement of 3D building models. In Proceedings of the 1st International Workshop on Next Generation 3D City Models (Vol. 1, No. 3.3).

Haala, N., & Kada, M. (2010). An update on automatic 3D building reconstruction. ISPRS Journal of Photogrammetry and Remote Sensing, 65(6), 570-580.

Maas, H. G., & Vosselman, G. (1999). Two algorithms for extracting building models from raw laser altimetry data. ISPRS Journal of photogrammetry and remote sensing, 54(2), 153-163.

Alharthy, A., & Bethel, J. (2002). Heuristic filtering and 3D feature extraction from LiDAR data. International Archives of Photogrammetry Remote Sensing and Spatial Information Sciences, 34(3/A), 29-34.

Alharthy, A., & Bethel, J. (2004, July). Detailed building reconstruction from airborne laser data using a moving surface method. In 20th Congress of International Society for Photogrammetry and Remote Sensing (pp. 213-218).

Arefi, H. (2008). Levels of detail in 3D building reconstruction from LiDAR data.

Kabolizade, M., Ebadi, H., & Mohammadzadeh, A. (2012). Design and implementation of an algorithm for automatic 3D reconstruction of building models using genetic algorithm. International Journal of Applied Earth Observation and Geoinformation, 19, 104-114.

Satari, M., Samadzadegan, F., Azizi, A., & Maas, H. G. (2012). A Multi-Resolution Hybrid Approach for Building Model Reconstruction from LiDAR Data. The Photogrammetric Record, 27(139), 330-359.

Mongus, D., Lukač, N., & Žalik, B. (2014). Ground and building extraction from LiDAR data based on differential morphological profiles and locally fitted surfaces. ISPRS Journal of Photogrammetry and Remote Sensing, 93, 145-156.

Song, J., Wu, J., & Jiang, Y. (2015). Extraction and reconstruction of curved surface buildings by contour clustering using airborne LiDAR data. Optik-International Journal for Light and Electron Optics, 126(5), 513-521.

Yu, Y., Liu, X., & Buckles, B. P. (2010, July). A cue line based method for building modeling from LiDAR and satellite imagery. In Computing Communication and Networking Technologies (ICCCNT), 2010 International Conference on (pp. 1-8). IEEE.

Awrangjeb, M., Fraser, C. S., & Lua, G. (2013, July). Integration of LiDAR data and orthoimage for automatic 3D building roof plane extraction. In Multimedia and Expo (ICME), 2013 IEEE International Conference on (pp. 1-6). IEEE.

Li, H., Zhong, C., Hu, X., Xiao, L., & Huang, X. (2013). New methodologies for precise building boundary extraction from LiDAR data and high resolution image. Sensor Review, 33(2), 157-165.

Arefi, H., & Reinartz, P. (2013). Building reconstruction using DSM and orthorectified images. Remote Sensing, 5(4), 1681-1703.

Haala, N., & Brenner, C. (1999). Extraction of buildings and trees in urban environments. ISPRS Journal of Photogrammetry and Remote Sensing, 54(2), 130-137.

Alexander, C., Smith-Voysey, S., Jarvis, C., & Tansey, K. (2009). Integrating building footprints and LiDAR elevation data to classify roof structures and visualise buildings. Computers, Environment and Urban Systems, 33(4), 285-292.

Kada, M., & McKinley, L. (2009). 3D building reconstruction from LiDAR based on a cell decomposition approach. International Archives of Photogrammetry, Remote Sensing and Spatial Information Sciences, 38(Part 3), W4.

Mian, A. S., Bennamoun, M., & Owens, R. A. (2004, December). Automatic multiview coarse registration of range images for 3D modeling. In Cybernetics and Intelligent Systems, 2004 IEEE Conference on (Vol. 1, pp. 158-163). IEEE.

Sajadian, M., & Arefi, H. (2014). A Data Driven Method for Building Reconstruction from LiDAR Point Clouds. The

International Archives of Photogrammetry, Remote Sensing and Spatial Information Sciences, 40(2), 225.

Fischler, M. A., & Bolles, R. C. (1981). Random Aample Consensus: a paradigm for model fitting with applications to image analysis and automated cartography. Communications of the ACM, 24(6), 381-395.